Chinese Chemical Letters 34 (2023) 107660

Contents lists available at ScienceDirect

Chinese Chemical Letters

journal homepage: www.elsevier.com/locate/cclet

Combined synthesis of interconvertible $Au_{11}Cd$ and $Au_{26}Cd_5$ for photocatalytic oxidations involving singlet oxygen

Jiafeng Zou[a,b], Wenwen Fei[a,b,*], Yao Qiao[a,b], Ying Yang[a,b], Zongbing He[a,b], Lei Feng[a,b], Man-Bo Li[a,b,*], Zhikun Wu[a,b,*]

[a] Institute of Physical Science and Information Technology, Anhui University, Hefei 230601, China
[b] Key Laboratory of Materials Physics, Anhui Key Laboratory of Nanomaterials and Nanotechnology, CAS Center for Excellence in Nanoscience, Institute of Solid State Physics, HFIPS, Chinese Academy of Sciences, Hefei 230031, China

ARTICLE INFO

Article history:
Received 19 March 2022
Revised 14 June 2022
Accepted 4 July 2022
Available online 6 July 2022

Keywords:
Gold nanoclusters
Cadmium-doping
Singlet oxygen
Photocatalysis
RLE-AGR

ABSTRACT

A novel $Au_{11}Cd$ nanocluster was synthesized by developing a combined method and controlling the kinetics, and another $Au_{26}Cd_5$ nanocluster was also obtained after the conditions were changed in the same reaction, which could transfer to $Au_{11}Cd$ in a two-way style. Both alloy nanoclusters can photocatalyze the production of singlet oxygen ($^1O_2$) and exhibit enhanced efficiencies in photocatalyzing two kinds of organic oxidations involving singlet oxygen compared with their non-alloyed mother nanoclusters, indicating that the Cd-doping might be an efficient way to enhance the photocatalysis performance of gold nanoclusters and metal nanoclusters are promising photocatalysts for organic oxidation involving singlet oxygen.

Metal nanoclusters (NCs) have attracted wide attention in recent years not only because of their well-defined compositions (structures) [1–6] but also because of their unique optical [7–13], magnetic [14–16], electrochemical [17–20], and catalytic properties [21–26]. However, the research of metal nanoclusters is still in its infancy. The research and application promotion are seriously dependent on the synthesis development for property improvement. In this context, a synthesis strategy [27] and a series of synthesis methods [28–31] have been proposed. Very recently, a reducing-ligand induction combined method [32] has been introduced, which provides implications for some other combination establishments. For example, the combination of "reverse ligand exchange (RLE)" [33] and "anti-galvanic reduction (AGR)" [30,34–38] is promising, because it may not only tune the compositions of NCs, but also enhance the NC properties (*e.g.*, stability, catalytic activity) and even lead to some new properties through the synergy of different metal atoms in the NCs. However, this combination is not widely realized yet, especially the combination with additional modulation of kinetics and thermodynamics has not been reported to the best of our knowledge. Developing the properties of NCs is also a current frontier research topic. To date, minimal work has shown that NCs can catalytically produce singlet oxygen ($^1O_2$) from O_2 under radiation and has exploited this property for photocatalytic oxidation reactions [39–45], which is important not only for improving oxidation selectivity but also for reducing energy consumption and pollution [46,47]. Recently, Zhuang *et al.* revealed that the doped Cd in gold nanoclusters by AGR is inclined to interact with O [48], and Agrachev *et al.* reported that cadmium-doping in gold NCs could enhance their photosensitive ability to produce $^1O_2$ [49], indicating that cadmium-doping might be a good choice for improving gold NCs performance in photocatalytic oxidation involving singlet oxygen. To test these conceits, we conducted this work starting from Au_{25} NCs, a benchmark of gold NCs, which will be described below.

Previous work has shown that excess PPh_3 can exchange the surface thiolate of gold nanoclusters. Because PPh_3 is a relatively weak protecting ligand for gold nanoclusters compared with thiolate, such an exchange was dubbed “reverse ligand exchange” (RLE). From a microscopic point of view, PPh_3 can break the "S-Au-S-Au-S" staple-like structures on the surface of gold nanoclusters and even change the conformation of the gold core to some extent, showing the "erosion" phenomenon. However, our earlier product was not easy to be purified with a meager yield [50]. Two independent processes were combined in this work: (i) RLE-erosion and (ii) AGR-doping. It was surprising that the difference in the degree of erosion step can directly lead to the difference in the final products. We chose a high concentration of PPh_3 and

* Corresponding authors at: Institute of Physical Science and Information Technology, Anhui University, Hefei 230601, China.
E-mail addresses: wenwen.fei@ahu.edu.cn (W. Fei), mbli@ahu.edu.cn (M.-B. Li), zkwu@issp.ac.cn (Z. Wu).

https://doi.org/10.1016/j.cclet.2022.07.003
1001-8417/

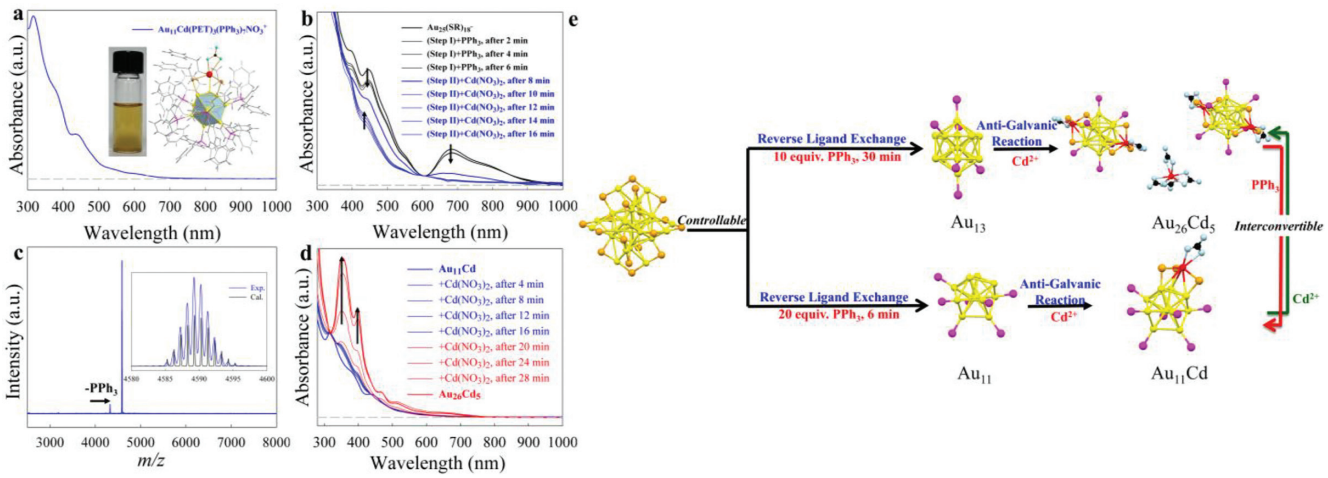

Fig. 1. (a) UV-vis-NIR spectrum of $Au_{11}Cd$ (Insets are the structure the photo of cluster solution). (b) UV-vis-NIR spectrum of samples taken at different times (see legends) during the synthesis of $Au_{11}Cd$. (c) ESI-MS spectrum of $Au_{11}Cd$, and the insets show the calculated (black) and experimental (blue) isotopic pattern (positive-mode). (d) UV-vis-NIR spectrum of samples taken at different times (see legends) during the transformation from $Au_{11}Cd$ (blue) to $Au_{26}Cd_5$ (red). (e) Routes of syntheses and structural transformations. Light yellow: Au; Orange: S; Magenta: P; Red: Cd; Black: N; Light Blue: O. The C and H atoms are omitted for clarity.

shorter erosion time (kinetical control) to synthesize a novel nanocluster (Fig. 1a) and the opposite for $Au_{26}Cd_5$ [50]. For the experimental details, see Supporting information. As shown in Fig. 1b and Fig. S1b (Supporting information), the three characteristic absorption peaks of $Au_{25}(SR)_{18}$ at ~400, ~450, ~680 nm began to weaken with the addition of PPh_3 in the two separate reactions. However, the different extents of erosion did not make noticeable differences in the UV-vis-NIR spectra. Proceeding to the second stage, we added the same dosages and concentrations of $Cd(NO_3)_2$ for the two reactions, and they went quickly in entirely different directions. As shown in Fig. 1b, the peaks belonging to $Au_{25}(SR)_{18}$ after deep erosion disappeared significantly within 8 min after the addition of Cd^{2+}. As the reaction proceeded, the characteristic absorption peaks at 390 and 440 nm belonging to a novel nanocluster gradually appeared, and the peak at 680 nm belonging to Au_{25} disappeared completely. After $Cd(NO_3)_2$ was added for *ca.* 16 min, the reaction tended to reach equilibrium, and the crude product was completely precipitated from toluene. It is noteworthy that since the two clusters are slightly soluble in toluene but better soluble in methanol, we chose toluene as the solvent in step I and introduced a moderate amount of methanol in step II. The adjustment of the solvent ratio reduces the difficulty of purification. Electrospray ionization mass spectrometry (ESI-MS) was employed to identify the molecular composition of the as-obtained product, and a dominant peak was observed at $m/z = 4589.23$ in the mass spectrum, which is assigned to $[Au_{11}Cd(PET)_3(PPh_3)_7NO_3]^+$ (Fig. 1c). For the other reaction with a relatively light degree of erosion, it can be found that all absorption peaks of $Au_{25}(SR)_{18}$ completely disappeared 10 min after the addition of $Cd(NO_3)_2$ (Fig. S1b in Supporting information). Still, new peaks were generated at 355 and 394 nm, which belong to $Au_{26}Cd_5$, and the doping reaction lasted about 40 min to the end. The major peak, corresponding to $[Au_{13}Cd_2(PET)_6(PPh_3)_6(NO_3)_2]^+$, was observed at $m/z = 5307.14$ (Fig. S1c in Supporting information) in the mass spectrum. Single crystal X-ray diffraction (SCXRD) confirmed their compositions $[Au_{11}Cd(PET)_3(PPh_3)_7NO_3]NO_3$ and $[Au_{13}Cd_2(PET)_6(PPh_3)_6(NO_3)_2]_2{\cdot}Cd(NO_3)_4$, respectively. The main structural frameworks of $Au_{11}Cd$ and $Au_{26}Cd_5$ are similar to those of Au_{11} and Au_{13}, respectively, and the Cd atom combines with three S atoms to form a "paw-like" motif structure attached to the outside of the gold core (Figs. S2 and S3 in Supporting information).

The structural transformation phenomena between the two nanoclusters have been discovered and monitored by UV-vis-NIR spectroscopy at room temperature. Fig. 1d shows the conversion from $Au_{11}Cd$ to $Au_{26}Cd_5$. The characteristic absorption of $Au_{11}Cd$ becomes weaker for 4 min after the addition of $Cd(NO_3)_2$. When the reaction proceeds to 12 min, it can be observed that the absorption peaks at 355 and 394 nm for $Au_{26}Cd_5$ start to show up in the UV-vis-NIR spectrum. The opposite transformation can be achieved by adding PPh_3 directly to $Au_{26}Cd_5$ (Fig. S1d in Supporting information). Compared with the former "bottom-up" conversion method, the latter "top-down" conversion process is significantly slower, taking more than 70 min to the equilibrium. The synthesis and structural transformation processes are shown in Fig. 1e.

$Au_{11}Cd$ and $Au_{26}Cd_5$ have subsequently been employed to photocatalyze the transformation from $^3O_2$ to $^1O_2$ (Fig. S4a in Supporting information). 1,3-Diphenylisobenzofuran (DPBF) was employed as the indicator since it can react with $^1O_2$ (Fig. S4b in Supporting information) and thus result in the notable absorption change. The absorption spectra of DPBF dissolved in $CHCl_3$ (bubbled with N_2 in advance) containing two separate nanoclusters under blue LED irradiation for 5, 10, and 20 s at room temperature are shown in Figs. S5a and S5c (Supporting information), respectively. The absorption band at 413 nm from DPBF decreased under irradiation, indicating the production of $^1O_2$, which was further confirmed by the electron spin resonance (ESR) experiments with 2,2,6,6-tetramethylpiperidine (TEMP) as a radical trapping agent (Figs. S4c, S5b, S5d and S6 in Supporting information).

After confirming the catalytical production of $^1O_2$, we started the photo-catalytic oxidation investigation. Sulfur has an abundance of oxidation states, and its redox processes also play a pivotal role in life [51,52]. Because of the interconversion of thioether, sulfoxide, and sulfone, the precise and controlled conversion between multiple valence states of sulfur is somehow challenging [53]. Herein, we demonstrated the highly selective oxidation of thioether to sulfoxide catalyzed by $Au_{11}Cd$ and $Au_{26}Cd_5$ under blue light irradiation (Fig. S7 in Supporting information). Both nanoclusters also displayed good stability in the presence of sulfide in $CHCl_3$, as shown in Fig. S8 (Supporting information). For comparison, Au_{25}, $Au_{24}Cd$, commercial-grade photosensitizer tetraphenyl porphyrin (TPP), $Cd(NO_3)_2$ and the mother nanoclusters Au_{11} and Au_{13} were also investigated, and the results are shown in Table S1 (Supporting information), which demonstrate: (i) the Cd-doping (including the case of Au_{25} doping) significantly improves the catalytic yield, especially, the Cd-doping of Au_{11} improves the catalytic yield by ~100%, manifesting that one-metal atom change of a nan-

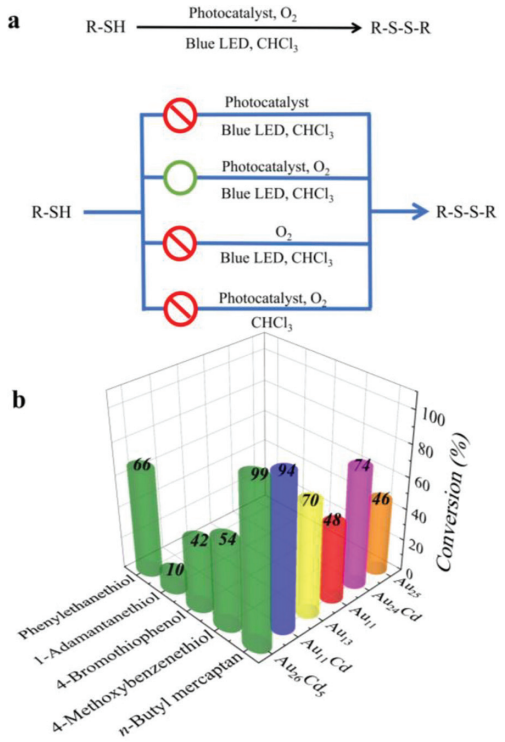

Fig. 2. (a) The impact of various parameters (light; O_2 and photocatalyst) on the disulfidation (red circle represents the inhibited reaction, while the green circle represents the smooth reaction). (b) Catalysis performance on different sulfur ligands with $Au_{26}Cd_5$, $Au_{11}Cd$, Au_{13}, Au_{11}, $Au_{24}Cd$, and Au_{25} as photocatalysts. Notes: The X, Y, Z-axis represent substrates, photosensitizers, and conversion of reactions, respectively. The values on the top of the cylinders represent the conversion of the reactions.

ocluster can dramatically influence its property. Such a dramatic enhancement is attributed to both electronic and atomic structure changes indicated by UV-vis-NIR spectrum (Fig. 1a) and SCXRD (Fig. S12a in Supporting information), respectively; (ii) metal nanoclusters are promising candidates for photocatalysts since only two nanoclusters among the investigated six nanoclusters were inferior to the commercial-grade photosensitizer TPP in terms of the conversion rate. To test the photocatalysis oxidation universality, some other reactions were also considered. Sulfhydryl ligands, including thiols and thiophenols, are susceptible to oxidation by different oxidizing agents, and disulfide is one kind of oxidation products [54]. The formation and breaking of disulfide bonds are essential in living organism metabolisms linked to enzyme-catalyzed redox. As a trial, $Au_{26}Cd_5$ was picked up for catalyzing phenylethanethiol to disulfide, with a > 99% selectivity, a *ca.* 66% conversion achieved (Table S2 in Supporting information).

EI-MS, ^{1}H-NMR, and ^{13}C-NMR confirmed the disulfide product (Figs. S13–S15 in Supporting information). Also, three sets of comparison experiments were carefully studied (Fig. 2a), and the results showed that the light, catalyst, and O_2 are all necessary, indicating the mentioned reaction is photocatalytic oxidation involving singlet oxygen. *n*-Butyl mercaptan, 1-adamantanethiol, 4-bromothiophenol, and 4–methoxybenzenethiol were further chosen as substrates for investigation (Fig. 2b), and the experimental results revealed that steric hindrance, as well as electron-withdrawing, has a negative influence on the catalysis efficiency. As a comparison, $Au_{26}Cd_5$, $Au_{11}Cd$, Au_{13}, Au_{11}, $Au_{24}Cd$, and Au_{25} were also tested for the selective oxidation of *n*–butyl mercaptan to a disulfide. The experimental results showed the same catalysis efficiency order: $Au_{26}Cd_5$ > $Au_{11}Cd$ > $Au_{24}Cd$ > Au_{13} > Au_{11} > Au_{25}, further indicating that the Cd-doping could enhance the photocatalytic oxidation efficiency of gold nanoclusters, given the consideration that $Au_{26}Cd_5$, $Au_{11}Cd$, and $Au_{24}Cd$ are the Cd-doping products of Au_{13}, Au_{11}, and Au_{25}, respectively. Among the investigated nanocluster catalysts, $Au_{26}Cd_5$ with the highest content of Cd achieved the best catalytic efficiency, which might also provide another support for the opinion that the Cd-doping promotes the photocatalysis of gold nanoclusters involving singlet oxygen. Further experiments reveal that the $Au_{26}Cd_5$ and $Au_{11}Cd$ are not very robust in some cases (Fig. S16 in Supporting information), which indicates that efforts might be made to improve the stability of such catalysts in the future.

In conclusion, a "RLE-AGR" combination method was developed to separately synthesize interconvertible $Au_{11}Cd$ and $Au_{26}Cd_5$ nanoclusters by controlling the reactions conditions (kinetics and thermodynamics). Both nanoclusters are precisely characterized by SCXRD, ESI-MS, *etc.*, and they show the interesting property for photocatalytic production of singlet oxygen ($^1O_2$) and exhibit enhanced efficiencies in selectively photocatalyzing thioether (sulfhydryl) oxidation compared with their non-alloyed mother nanoclusters, indicating that the Cd-doping might promote the photocatalytic performance of gold nanoclusters. By comparing the photocatalysis efficiencies of nanoclusters with that of a commercial-grade photosensitizer TPP, we revealed that metal nanoclusters are tunable and promising photocatalysts for organic oxidation involving singlet oxygen. Overall, our work has important implications for the syntheses, properties, and applications of nanoclusters, and is expected to stimulate more work in related fields.

Declaration of competing interest

The authors declare no conflict of interest.

Acknowledgments

Fei thanks the startup funds from Anhui University (No. S020318006/022). We acknowledge the financial support from the National Natural Science Foundation of China (Nos. 92061110, 21829501, 21925303, 21771186, 21222301, 21528303 and 21171170), Anhui Provincial Natural Science Foundation (No. 2108085Y05), Hefei National Laboratory for Physical Sciences at the Microscale (No. KF2020102) and Innovative Program of Development Foundation of Hefei Center for Physical Science and Technology (No. 2020HSC-CIP005).

Supplementary materials

Supplementary material associated with this article can be found, in the online version, at doi:10.1016/j.cclet.2022.07.003.

References

[1] P.D. Jadzinsky, G. Calero, C.J. Ackerson, et al., Science 318 (2007) 430–433.
[2] M.W. Heaven, A. Dass, P.S. White, et al., J. Am. Chem. Soc. 130 (2008) 3754–3755.
[3] M. Zhu, C.M. Aikens, F.J. Hollander, et al., J. Am. Chem. Soc. 130 (2008) 5883–5885.
[4] C.P. Joshi, M.S. Bootharaju, M.J. Alhilaly, et al., J. Am. Chem. Soc. 137 (2015) 11578–11581.
[5] Z. Lei, J.J. Li, Z.A. Nan, et al., Angew. Chem. Int. Ed. 60 (2021) 14415–14419.
[6] X. Zhang, H.Y. Yang, X.J. Zhao, et al., Chin. Chem. Lett. 25 (2014) 839–843.
[7] Q. Li, M. Zhou, W.Y. So, et al., J. Am. Chem. Soc. 141 (2019) 5314–5325.
[8] Y. Yu, Z. Luo, D.M. Chevrier, et al., J. Am. Chem. Soc. 136 (2014) 1246–1249.
[9] M.M. Zhang, X.Y. Dong, Z.Y. Wang, et al., J. Am. Chem. Soc. 143 (2021) 6048–6053.
[10] E.B. Guidez, C.M. Aikens, Nanoscale 4 (2012) 4190–4198.
[11] S.H. Yau, O. Varnavski, T. Goodson, Acc. Chem. Res. 46 (2013) 1506–1516.
[12] M.R. Narouz, S. Takano, P.A. Lummis, et al., J. Am. Chem. Soc. 141 (2019) 14997–15002.
[13] X.M. Fu, X.Z. Lin, X.Q. Ren, et al., Chin. Chem. Lett. 32 (2021) 565–568.
[14] R.S. McCoy, S. Choi, G. Collins, et al., ACS Nano 7 (2013) 2610–2616.

[15] M. Zhu, C.M. Aikens, M.P. Hendrich, et al., J. Am. Chem. Soc. 131 (2009) 2490–2492.
[16] Y. Negishi, H. Tsunoyama, M. Suzuki, et al., J. Am. Chem. Soc. 128 (2006) 12034–12035.
[17] S.S. Kumar, K. Kwak, D. Lee, Electroanalysis 23 (2011) 2116–2124.
[18] W. Chen, S. Chen, Angew. Chem. Int. Ed. 48 (2009) 4386–4389.
[19] S. Antonello, F. Maran, Curr. Opin. Electrochem. 2 (2017) 18–25.
[20] L. He, J. Yuan, N. Xia, et al., J. Am. Chem. Soc. 140 (2018) 3487–3490.
[21] R. Jin, G. Li, S. Sharma, et al., Chem. Rev. 121 (2021) 567–648.
[22] Y. Sun, X. Liu, K. Xiao, et al., ACS Catal. 11 (2021) 11551–11560.
[23] G. Li, R. Jin, J. Am. Chem. Soc. 136 (2014) 11347–11354.
[24] M. Zhao, S. Huang, Q. Fu, et al., Angew. Chem. Int. Ed. 59 (2020) 20031–20036.
[25] C. Li, O.J.H. Chai, Q. Yao, et al., Mater. Horiz. 8 (2021) 1657–1682.
[26] Z.L. Wu, D.R. Mullins, L.F. Allard, et al., Chin. Chem. Lett. 29 (2018) 795–799.
[27] Z. Wu, M.A. MacDonald, J. Chen, et al., J. Am. Chem. Soc. 133 (2011) 9670–9673.
[28] Z. Wu, J. Suhan, R. Jin, J. Mater. Chem. 19 (2009) 622–626.
[29] C. Zeng, H. Qian, T. Li, et al., Angew. Chem. Int. Ed. 51 (2012) 13114–13118.
[30] Z. Wu, Angew. Chem. Int. Ed. 51 (2012) 2934–2938.
[31] K.R. Krishnadas, A. Ghosh, A. Baksi, et al., J. Am. Chem. Soc. 138 (2015) 140–148.
[32] J. Dong, Z. Gan, W. Gu, et al., Angew. Chem. Int. Ed. 60 (2021) 17932–17936.
[33] M.B. Li, S.K. Tian, Z. Wu, et al., Chem. Mater. 28 (2016) 1022–1025.
[34] M. Wang, Z. Wu, Z. Chu, et al., Chem. Asian J. 9 (2014) 1006–1010.
[35] L. Liao, S. Zhou, Y. Dai, et al., J. Am. Chem. Soc. 137 (2015) 9511–9514.
[36] C. Yao, Y.J. Lin, J. Yuan, et al., J. Am. Chem. Soc. 137 (2015) 15350–15353.
[37] Z. Gan, N. Xia, Z. Wu, Acc. Chem. Res. 51 (2018) 2774–2783.
[38] N. Yan, L. Liao, J. Yuan, et al., Chem. Mater. 28 (2016) 8240–8247.
[39] H. Kawasaki, S. Kumar, G. Li, et al., Chem. Mater. 26 (2014) 2777–2788.
[40] Z. Li, C. Liu, H. Abroshan, et al., ACS Catal. 7 (2017) 3368–3374.
[41] J. Liao, K. Li, H. Ma, et al., Chin. Chem. Lett. 31 (2020) 2737–2741.
[42] T. Hou, Z. Gao, J. Zhang, et al., Trans. Tianjin Univ. 27 (2021) 331–337.
[43] Y.N. Jang, Z.K. Xiong, J.B. Huang, et al., Chin. Chem. Lett. 33 (2022) 415–423.
[44] Y. Zhou, J. He, J. Lu, et al., Chin. Chem. Lett. 31 (2020) 2623–2626.
[45] G.M. Zhang, R.R. Wang, G. Li, Chin. Chem. Lett. 29 (2018) 687–693.
[46] C. Liu, X. Ren, F. Lin, et al., Angew. Chem. Int. Ed. 58 (2019) 11335–11339.
[47] Y. Nosaka, A.Y. Nosaka, Chem. Rev. 117 (2017) 11302–11336.
[48] S. Zhuang, D. Chen, L. Liao, et al., Angew. Chem. Int. Ed. 132 (2020) 3097–3101.
[49] M. Agrachev, W. Fei, S. Antonello, et al., Chem. Sci. 11 (2020) 3427–3440.
[50] M.B. Li, S.K. Tian, Z. Wu, Chin. J. Chem. 35 (2017) 567–571.
[51] A. Gomes, E. Fernandes, J.L. Lima, J. Biochem. Biophys. Methods 65 (2005) 45–80.
[52] H. Xu, Y.F. Zhang, X.J. Lang, Chin. Chem. Lett. 31 (2020) 1520–1524.
[53] X. Feng, X. Wang, H. Wang, et al., ACS Appl. Mater. Interfaces 11 (2019) 45118–45125.
[54] Y. Saito, Y. Shichibu, K. Konishi, Nanoscale 13 (2021) 9971–9977.